Available online at www.sciencedirect.com
SCIENCE DIRECT®
Journal of Marine Systems 60 (2006) 365 – 380
JOURNAL OF MARINE SYSTEMS
www.elsevier.com/locate/jmarsys

Using a random displacement model to simulate turbulent particle motion in a baroclinic frontal zone: A new implementation scheme and model performance tests

E.W. North *, R.R. Hood, S.-Y. Chao, L.P. Sanford

University of Maryland Center for Environmental Science, Horn Point Laboratory, P.O. Box 775, Cambridge, MD 21613, USA

Received 11 February 2005; accepted 24 August 2005
Available online 5 April 2006

Abstract

Numerical artifacts can limit accurate simulation of turbulent particle motion when Lagrangian particle-tracking models are implemented in hydrodynamic models with stratified conditions like fronts. Yet, modeling of individual particle motion in frontal regions is critical for understanding sediment dynamics as well as the transport and retention of planktonic organisms. The objective of this research was to develop a numerical technique to accurately simulate turbulent particle motions in a particle-tracking model embedded within a hydrodynamic model of a frontal zone. A new interpolation scheme, the 'water column profile' scheme, was developed and used to implement a random displacement model for turbulent particle motions. A new interpolation scheme was necessary because linear interpolation schemes caused artificial aggregation of particles where abrupt changes in vertical diffusivity occurred. The new 'water column profile' scheme was used to fit a continuous function (a tension spline) to a smoothed profile of vertical diffusivities at the *x–y* particle location. The new implementation scheme was checked for artifacts and compared with a standard random walk model using (1) Well Mixed Condition tests, and (2) dye-release experiments. The Well Mixed Condition tests confirmed that the use of the 'water column profile' interpolation scheme for implementing the random displacement model significantly reduced numerical artifacts. In dye-release experiments, high concentrations of Eulerian tracer and Lagrangian particles were released at the same location up-estuary of the salt front and tracked for 4 days. After small differences in initial dispersal rates, tracer and particle distributions remained highly correlated ($r=0.84$ to 0.99) when a random displacement model was implemented in the particle-tracking model. In contrast, correlation coefficients were substantially lower ($r=0.07$ to 0.58) when a random walk model was implemented. In general, model performance tests indicated that the 'water column interpolation' scheme was an effective technique for implementing a random displacement model within a hydrodynamic model, and both could be used to accurately simulate diffusion in a highly baroclinic frontal region. The new implementation scheme has the potential to be a useful tool for investigating the influence of hydrodynamic variability on the transport of sediment particles and planktonic organisms in frontal zones.

Keywords: Lagrangian particle-tracking modeling; Fronts; Mathematical models; Biological–physical interactions

* Corresponding author. Tel.: +1 410 221 8497; fax: +1 410 221 8490.
E-mail address: enorth@hpl.umces.edu (E.W. North).

0924-7963/$ - see front matter © 2006 Elsevier B.V. All rights reserved.
doi:10.1016/j.jmarsys.2005.08.003

1. Introduction

Lagrangian particle-tracking models coupled with hydrodynamic models have been used successfully to understand the influence of physical conditions on dispersal, growth, and survival of planktonic organisms (Werner et al., 1996; Hannah et al., 1998; Heath and Gallego, 1998; Hare et al., 1999; Hood et al., 1999; Bartsch and Coombs, 2001; Hinckley et al., 2001; Werner et al., 2001; Hinrichsen et al., 2003; Brown et al., 2004). Few of these models have been applied to investigate biological–physical interactions in estuarine or plume fronts where baroclinicity presents a numerical challenge for particle–tracking models (Visser, 1997; Brickman and Smith, 2002). Yet, fronts are an important area of research. Fronts structure physical conditions such as temperature, salinity, and sediment and nutrient concentrations (Largier, 1993) as well as the distribution of planktonic organisms including phytoplankton, crustacean zooplankton, and fish larvae (Jillett and Zeldis, 1985; Epifanio, 1987; Mackas and Louttit, 1988; Govoni et al., 1989; Hood et al., 1991; Govoni and Grimes, 1992; Uye et al., 1992; Govoni, 1993; Kingsford and Suthers, 1996; Franks and Walstad, 1997; Okazaki et al., 1998; Munk et al., 1999; Nakata et al., 2000; Shanks et al., 2000; Epstein and Beardsley, 2001; Lough and Manning, 2001; Bjorkstedt et al., 2002; Munk et al., 2002; North and Houde, 2004). Frontal regions are important areas for plankton growth due to enhanced nutrient concentrations and convergent circulation that can promote production, increase aggregation of organisms, and intensify trophic interactions (Wolanski and Hamner, 1988; Boynton et al., 1997; Winkler et al., 2003; Roman et al., 2005).

The salt front (landward margin of salinity intrusion) at the head of estuaries is an ideal test case to advance numerical approaches and enhance our understanding of biological–physical interactions in frontal regions. Strong baroclinicity and associated gradients in turbulence present a numerical challenge for particle-tracking models (Brickman and Smith, 2002). Nevertheless, improving coupled biological–physical models in this region will enable enhanced understanding of the factors that affect fish recruitment. Field evidence suggests that physical conditions near the salt front may have a strong influence on anadromous larval fish survival and juvenile recruitment (North and Houde, 2001, 2003). Circulation patterns in this region can create an estuarine turbidity maximum (ETM) that is characterized by elevated turbidity and suspended sediment concentrations compared to those up- and down-estuary (Schubel, 1968). ETMs are found in coastal plain estuaries throughout the world, including estuaries in Canada, France, Germany, UK, and USA (Schubel, 1968; Allen et al., 1980; D'Anglejan, 1981; Uncles and Stephens, 1993; Jay and Musiak, 1994; Burau et al., 1998; Geyer et al., 2001; Kappenberg and Grabemann, 2001; Lin and Kuo, 2001; Sanford et al., 2001; Kostaschuk, 2002). The ETM region is an important nursery area for larval fish in the St. Lawrence River estuary (Dodson et al., 1989; Dauvin and Dodson, 1990; Sirois and Dodson, 2000), the San Francisco Bay/Delta (Jassby et al., 1995; Bennett et al., 2002), and upper Chesapeake Bay (Boynton et al., 1997; North and Houde, 2001, 2003). The numerical hydrodynamic model employed in this research reproduces a salt front and ETM (North et al., 2004).

Particle-tracking models include a sub-grid scale turbulence model to simulate turbulent motion at scales smaller than those resolved by the hydrodynamic model. When implemented in hydrodynamic models that contain sharp gradients in turbulence (e.g., fronts), the standard sub-grid scale turbulence model (random walk model) causes artificial aggregation of neutrally buoyant particles in areas of low diffusivity, violating the Well Mixed Condition (Visser, 1997; Brickman and Smith, 2002). Particle-tracking models that adhere to the Well Mixed Condition maintain "an initially uniform concentration of [neutrally buoyant] particles uniform for all time" (Brickman and Smith, 2002).

Our objective was to develop a particle-tracking model that successfully simulated turbulent particle motion in highly baroclinic frontal regions using a random displacement model. We describe a new interpolation scheme for implementing a random displacement model in a coupled hydrodynamic-particle-tracking model and summarize results of two model performance assessments: (1) 2D Well Mixed Condition tests to detect numerical artifacts, and (2) dye-release experiments to determine if the sub-grid scale turbulence model adequately simulates diffusion. In addition, we present results of 1D numerical studies that provide guidance on implementing the new interpolation scheme in hydrodynamic models with gradients in turbulence.

2. Methods

2.1. Hydrodynamic and sediment transport model

The three-dimensional hydrodynamic ETM model was based on the code of the Princeton Ocean Model (POM) under hydrostatic and Boussinesq approximations (Blumberg and Mellor, 1987; Mellor, 1998). Eddy viscosity and diffusivity were determined by the level-2.5 turbulent closure scheme of Mellor and Yamada (1974). Our enhancements to POM included building suspended sediment and sediment transport components, adding constant loading of suspended sediment at the up-stream boundary, parameterizing bottom sediment burial with a Newtonian dampening term, and constructing a more reasonable formulation for background vertical diffusivity. Detailed information about these enhancements and hydrodynamic model parameterization and boundary conditions can be found in North et al. (2004).

The ETM model domain (Fig. 1) contained a 98-km-long and 4.8-km-wide channel with a gradually widening seaward reservoir that was 2237 km long and had a maximum width of 66 km. The entire basin was 12 m deep and contained 145-grid spacings in the x-direction (seaward) and 6 in the y-direction (across channel). Vertical resolution was provided by 12 σ-coordinate layers. In the first 98 km of the channel, the longitudinal resolution (Δx) was 1 km and the lateral resolution (Δy) was 0.8 km. In the seaward reservoir, Δx and Δy gradually increased at a rate of 12% and 5.5% per grid, respectively. The seaward reservoir, although of minor importance to the circulation and sediment transport within the channel, served as a buffer zone to enhance the long-term computational stability of the model. The temporal resolution of the model was split. Vertically averaged currents and sea level were resolved with a time step of 5 s, and salinity, sediment concentration, and vertically explicit current velocities were resolved with a time step of 40 s.

A barotropic tidal generation force was included in the longitudinal momentum equation to produce semidiurnal tidal currents in the channel. Tidal current speed and upstream dissipation were parameterized so that sea level height and tidal current velocities in the model were similar to those of predicted tides in upper Chesapeake Bay. Lateral walls bounding the channel were impenetrable, impermeable and free-slip.

Initially, the model channel was filled with motionless clear water of 12 practical salinity units (psu) and there was no sediment at the bottom of the basin. The model was run with river inflow = 0.07 m s^{-1} and constant sediment loading until the model reached a quasi steady state at day 350 (Fig. 2a). In this quasi steady state, sediment input equaled sediment burial and the location of the salt front was stable: it oscillated with the tidal current in a repetitive cycle but did not progress up or down estuary. All model scenarios herein used the quasi steady-state solution at day 350 as the initial condition.

2.2. Particle-tracking model formulation

The Lagrangian particle-tracking model was constructed as a subroutine of the hydrodynamic model that was called every internal time step (40 s). Current velocity, sea surface height, and horizontal and vertical diffusivity derived in the hydrodynamic model were passed to the particle-tracking model. Changes in particle locations due to advection were calculated every 10 s using a 'water column profile' interpolation scheme (Section 2.2.1) to estimate velocity at each particle location. Near the bottom, the law-of-the-wall was applied so that u-, v-, and w-current velocities decreased logarithmically to the depth of the roughness height (0.001 m). Changes in particle locations due to turbulence were updated every 1 s using a random walk model in the horizontal (Section 2.2.2) and a random displacement model in the vertical (Section 2.2.3).

2.2.1. Interpolation scheme

In the 'water column profile' interpolation scheme, modeled velocities and diffusivities were interpolated horizontally (4-point linear interpolation) at each sigma

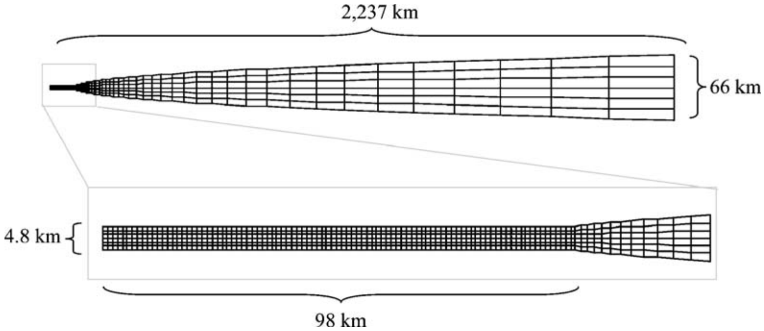

Fig. 1. Schematic of model domain. Upper diagram represents the entire model domain. Lower diagram illustrates the grid line geometry of the channel, the region of interest.

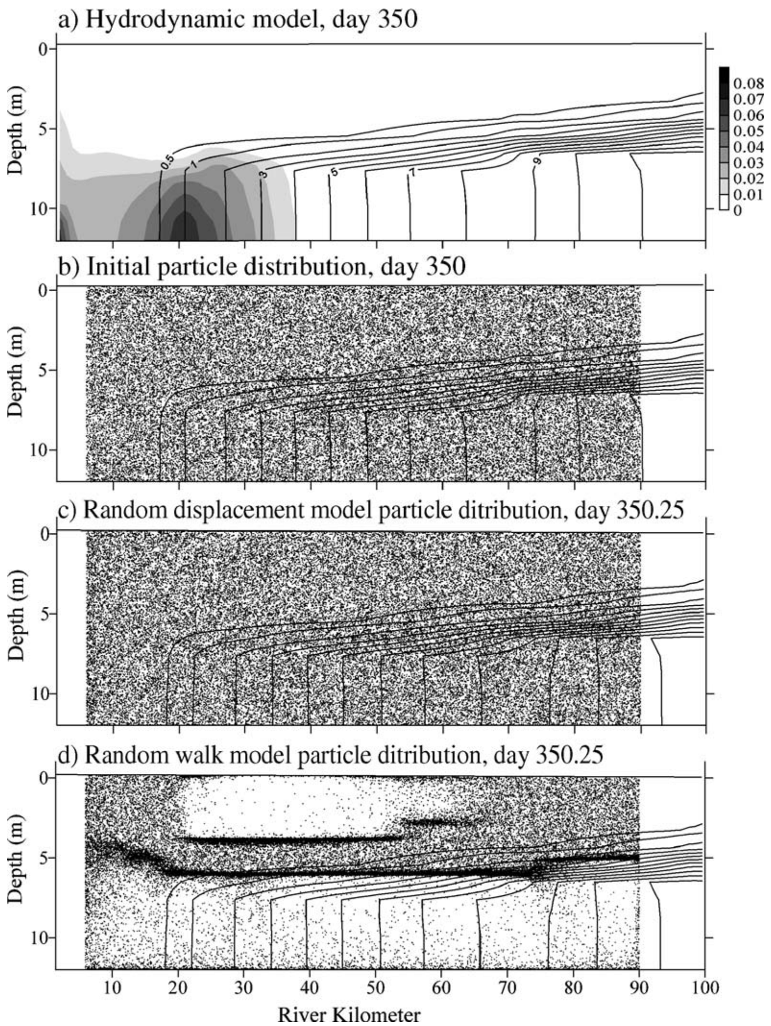

Fig. 2. Hydrodynamic model output and particle distributions. (a) Hydrodynamic model output at day 350. Line contours are salinity and shaded contours are suspended sediment concentrations (kg m^{-3}, color scale on right). (b) Initial position of 50,000 particles randomly distributed throughout the particle-tracking model domain. (c) Particle distribution after 6 h when a random displacement model was used to simulate sub-grid scale turbulence in the vertical direction. (d) Particle distribution after 6 h when a random walk model was used to simulate sub-grid scale turbulence in the vertical direction.

level to create a vertical profile of values at the *x–y* particle location (Fig. 3a). For current velocities, a tension spline curve was fit to the vertical profile (Fig. 3b) and was used to estimate current velocity at the particle location, except near bottom where the law-of-the-wall was applied. To implement the random displacement model (Section 2.2.3), two steps were added to the 'water column profile' interpolation scheme to estimate vertical diffusivity (K_v) and its derivative (K_v') at the particle location. After the water column profile of vertical diffusivity at the *x–y* particle location was constructed (Fig. 3a), the number of data points between sigma layers was proliferated with linear interpolation. Then, an 8-point moving average was used to smooth the data (Fig. 3c) before fitting the tension spline curve. Surface and bottom boundary values were forced to equal minimum vertical diffusivity in the hydrodynamic model after smoothing was complete.

Tension splines do not add extraneous inflection points (like simple spline curves), and preserve the local shape of the data (monotonicity and convexity). Tension spline curves were fit using a subroutine and functions from the Tension Spline Curve Fitting Package (TSPACK). TSPACK (TOMS/716) was created by Robert J. Renka (renka@cs.unt.edu, Department of Computer Science and Engineering, University of North Texas) and is available for download from http://www.

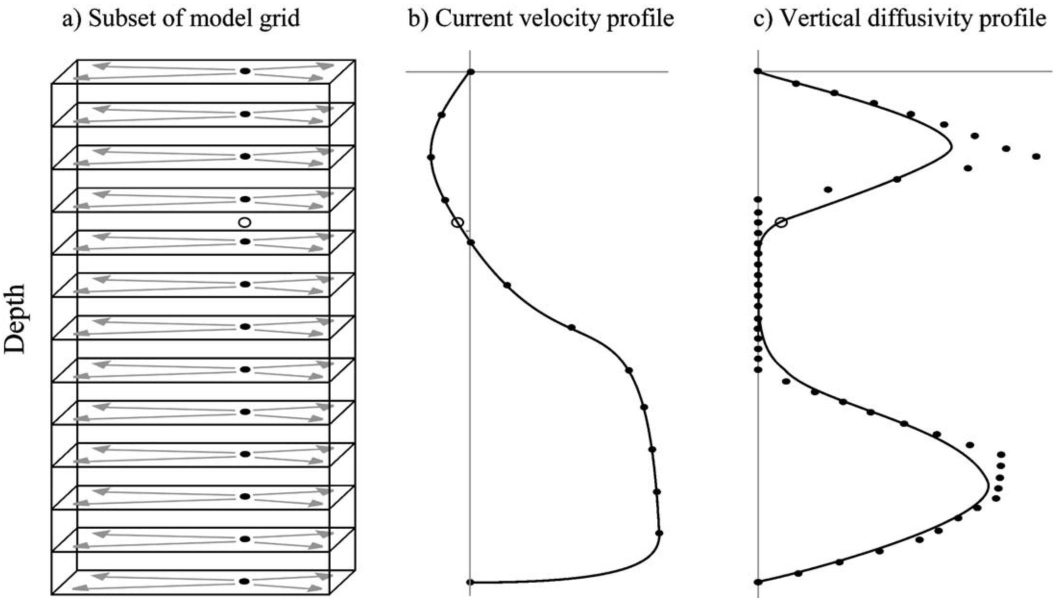

Fig. 3. Schematic of interpolation scheme for particle-tracking model. (a) Subset of model grid. Hydrodynamic model output was interpolated at each sigma level to create a vertical profile (closed circles) at the x–y particle location (open circles) using 4-point linear interpolation (gray arrows). (b) Profile of along-channel current velocity. A tension spline (line) was fit to the vertical profile of along-channel current velocity values (filled circles) and used to estimate velocity at the particle location (open circle). Law-of-the-wall was applied near bottom. (c) Profile of vertical diffusivity. Data points were proliferated with linear interpolation (filled circles), smoothed with an 8-point moving average, and fit with a tension spline (line) in order to estimate vertical diffusivity at the particle location (open circle).

netlib.org. Occasionally, the curve fitting method would fail to converge (~0.0004% of the time, or once in 244,500 calls to TSPACK). In these rare cases, simple linear interpolation of the vertical profile was used to avoid program pause.

2.2.2. Horizontal turbulence

Because the hydrodynamic model was tuned to examine along-channel processes, sub-grid scale turbulence in the cross-channel direction was omitted from the particle-tracking model. A random walk model (Visser, 1997) was implemented within the particle-tracking model to simulate sub-grid scale turbulence in the along-channel direction (x):

$$x_{n+1} = x_n + R[2d^{-1}K_h\delta t]^{1/2} \quad (1)$$

where x_n = initial particle location, K_h = horizontal diffusivity at the particle location, δt = time step of the random walk model (δt = 1 s), and R is a random process with mean = 0 and standard deviation d = 1. A random walk model was used to represent sub-grid scale turbulence in the horizontal direction because we used constant horizontal diffusivity in the ETM model. In situations with constant diffusivity, random walk and random displacement models are equivalent (Visser, 1997).

2.2.3. Vertical turbulence

A random displacement model (Visser, 1997) was implemented within the particle-tracking model to simulate sub-grid scale turbulence in the vertical (z) direction:

$$z_{n+1} = z_n + K_v'\delta t + R[2d^{-1}K_v\delta t]^{1/2} \quad (2)$$

where z_n = initial particle location, K_v = vertical diffusivity evaluated at ($z_n + 0.5K_v'\delta t$), δt = time step of the random displacement model, $K_v' = \partial K_v/\partial z$ evaluated at z_n, and R is a random process with mean = 0 and standard deviation d = 1. To satisfy the random displacement model criterion $\delta t \ll \min(1/K_v'')$ (Visser, 1997), the time step (δt) was set at 1 s after examination of a 10-d time series of $1/K_v''$ that included wind events. When K_v' = 0, the random displacement model (Eq. (2)) reduces to a random walk model (Eq. (1)).

The random displacement model was found to be most sensitive to parameterization of the second term, the gradient in vertical diffusivity at the particle location (K_v'). Many methods were used to estimate K_v' at the particle location, including 8-point linear interpolation, proliferating data points and smoothing the vertical diffusivity profile with moving averages, and fitting simple spline curves. All linear interpolation schemes caused artificial aggregation of particles near sharp changes in diffusivity, even after data points were smoothed. These results support the conclusions of Brickman and Smith (2002) who found that discontinuities in the vertical profile of K_v made demonstration of the Well Mixed Condition impossible. Although simple spline curves resulted in smooth functions, they caused artificial gaps in particle distributions because of added inflection points near sharp changes in vertical diffusivity. The best results were obtained by fitting a tension spline to a smoothed water column profile of vertical diffusivity at the particle location as described in Section 2.2.1.

2.2.4. Vertical boundary conditions

Reflective boundary conditions were specified for the surface and bottom boundaries (Proehl and Lynch, 2001; Brickman and Smith, 2002). If a particle passed through the surface or bottom boundary due to turbulence or vertical advection, the particle was placed back in the model domain at a distance from the boundary equal to the distance that the particle location exceeded the boundary. In models with sinking particles, if sinking caused a particle to pass through the bottom boundary, the particle was placed at the boundary. If turbulence or vertical advection caused a sinking particle to pass through the boundary, the particle was placed back in the model domain at a distance from the boundary equal to the distance that the particle location exceeded the boundary (i.e., it was reflected).

2.2.5. Horizontal boundary conditions

Advection was the dominant transport process in the hydrodynamic model. Horizontal boundary conditions differed between model performance tests due to the effects of advection and the requirements of the test. For tests of the Well Mixed Condition, particles needed to be retained within the bounds of the particle-tracking model (6 to 90 river km of the hydrodynamic model) and not advected down- or up-estuary. To maintain particles within the particle-tracking model boundary, particles were 'looped' between boundaries. If a particle hit the up-estuary boundary, it was placed at the down-estuary boundary at a randomly assigned depth, and vice versa.

For the dye-release experiments, the horizontal boundaries needed to encompass the area of tracer dispersal apparent in the Eulerian model. Therefore the particle-tracking model boundaries were expanded (1.5 to 97 river km). In the rare event that a particle contacted the up- or down-estuary boundary, the particle location was simply maintained at that boundary.

2.3. 2D Well Mixed Condition Test

For tests of the Well Mixed Condition (WMC), 100,000 particles were released in an initially random distribution in a x–z plane in the center of the channel (similar to Fig. 2b) and tracked over 1 tidal cycle (12 h) during steady-state conditions. In the WMC scenarios presented here, the number of particles in each grid cell was ~90, a number that resulted in acceptable variance in the Lagrangian solution and allowed reasonable computation time (Proehl and Lynch, 2001). Five 12-h scenarios were conducted with a random displacement model to simulate sub-grid scale turbulence in the vertical direction. The five scenarios were identical except that the initial location of particles differed (i.e., a different snapshot random distribution of 100,000 particles was used as the initial condition for each scenario). For comparison, the same scenarios were repeated with a random walk model implemented to simulate vertical turbulent motion.

A quantitative measure of the WMC was adapted from Brickman and Smith (2002). The 2D WMC correlation test was based on the expected lack of association between particle concentrations and vertical diffusivity. If particles aggregated in regions of low diffusivity (e.g. Fig. 2d), then a negative correlation between particle concentrations and K_v would result, indicating violation of the WMC. If there was no significant correlation between K_v and particle concentrations over time, then the WMC was demonstrated.

The procedure for the 2D correlation test had two parts: (1) calculating correlation coefficients from model output and (2) conducting the significance tests. To calculate correlation coefficients from model output, the concentration of particles in a box surrounding each K_v hydrodynamic grid point was calculated and used to compute the correlation between particle concentrations and K_v in the x–z plane in the center of the channel (SAS version 8.01). Although Brickman and Smith (2002) computed Pearson's correlation coefficients, Spearman's rank-order correlation coefficients (r) were used here because K_v values from the hydrodynamic model were not normally distributed. Correlation coefficients of model output were calculated every 0.25 h for each 12-h model run.

The first step of the significance tests was to conduct correlation tests between randomly distributed particle concentrations and K_v values (after Brickman and Smith, 2002). Two thousand snapshot distributions of 100,000 particles were generated by randomly placing particles throughout the particle-tracking model domain. The correlation between particle concentration and vertical diffusivity (K_v) was calculated at a single time point for each of the 2000 random distributions. Of the 2000 correlation coefficients, the 2.5th and 97.5th percentile values were selected as bounds for 95% confidence intervals (Brickman and Smith, 2002) and the maximum and minimum r values were selected as the upper and lower bounds of the non-significant range. This procedure was repeated every 0.25 h for 12 h to determine the 95% confidence intervals and the non-significant range over time.

The second step of the significance tests was to compare the correlation coefficients from each model scenario's output to the 95% confidence limits and the non-significant range. If they were outside the non-significant range, then model correlation coefficients were considered significantly different from those of randomly distributed particles and in violation of the WMC. If model correlation coefficients remained within the non-significant range over time, then the WMC was considered satisfied.

2.4. Dye-release experiments

Model dye-release experiments were conducted to determine if the particle-tracking model predictions agreed with simulated diffusion. Eulerian tracer (i.e., the ‘dye’) and Lagrangian particles were released at the same location and tracked over time. Similar evolution of tracer and particle distributions indicated that the Lagrangian particle-tracking model adequately simulated diffusion.

To adapt the ETM hydrodynamic model to dye release studies: (1) subroutines that calculate suspended sediment concentrations were converted to neutrally buoyant or slowly sinking tracers that did not affect water density; (2) the tracer was not allowed to deposit on the bottom; and (3) no tracer was allowed to enter from the up-estuary boundary.

In dye-release experiments, high concentrations of an Eulerian tracer and 20,000 neutrally buoyant particles were released in the same grid cell in the center of the hydrodynamic model channel. The model was run for 4 days and the concentrations of particles and tracer in each hydrodynamic grid cell in the center of the channel were compared graphically and with Pearson's correlation tests (SAS version 8.01). Scenarios were conducted with neutrally buoyant particles and tracer as well as those with the same constant sinking speed similar to small sediment particles ($0.03\,\mathrm{mm\,s^{-1}}$). In addition, neutrally buoyant and sinking tracer/particle scenarios were repeated with and without a wind event that started on day 350.125 and ended on day 352 (21 h). The wind event was simulated by applying a down-estuary wind stress of $1.66\,\mathrm{dyn\,cm^{-2}}$ (approximately $9.1\,\mathrm{m\,s^{-1}}$ wind speed). In all cases, the scenarios were repeated twice, once with a random displacement model implemented in the particle-tracking model, and once with a random walk model. The number of particles used in the dye-release studies was determined by examining the mean and variance of model correlation coefficients versus number of particles released. The lowest number of particles that resulted in a stable mean with little variance (20,000 particles) was selected for the dye-release experiments (Fig. 4). Each mean and variance value in Fig. 4 was calculated with the Pearson's correlation coefficients of particle concentrations versus tracer concentrations at day 352 for 5 dye-release simulations. The 5 simulations were conducted with identical models except that different seed values were used to initialize the random number generator.

2.5. 1D smoothing experiments

1D numerical studies were conducted to provide guidance on the degree of smoothing to implement when applying the water column interpolation scheme in hydrodynamic models with gradients in turbulence. A series of 1D models was constructed with (1) vertical profiles that included simple gradients in vertical diffusivity and (2) particle-tracking models implemented with different levels of smoothing in the water column profile interpolation scheme. Models were initialized with randomly distributed particles and run for 12 h after which a 1D WMC test was conducted to determine if the particles remained uniformly distributed.

1D profiles of vertical diffusivity were constructed with a gradient from 6 to 7 m and with uniform diffusivities from 0 to 6 m and from 7 to 13 m. Two profile types were created: (1) profiles with high uniform vertical diffusivities in the bottom layer and low vertical diffusivities in the surface layer, and (2) profiles with the reverse (low values in the bottom layer; high values in the surface layer). The low value of vertical diffusivity was fixed at $5.0\times10^{-7}\,\mathrm{m^2\,s^{-1}}$ in all models. The high value was varied from 5.0×10^{-6} to $0.09\,\mathrm{m^2\,s^{-1}}$ to create 33 profiles with gradients in vertical diffusivity ($K_v'=\partial K_v/\partial z$) that ranged from 4.5×10^{-6} to $8.99995\times10^{-2}\,\mathrm{m^2\,s^{-1}}$ per m.

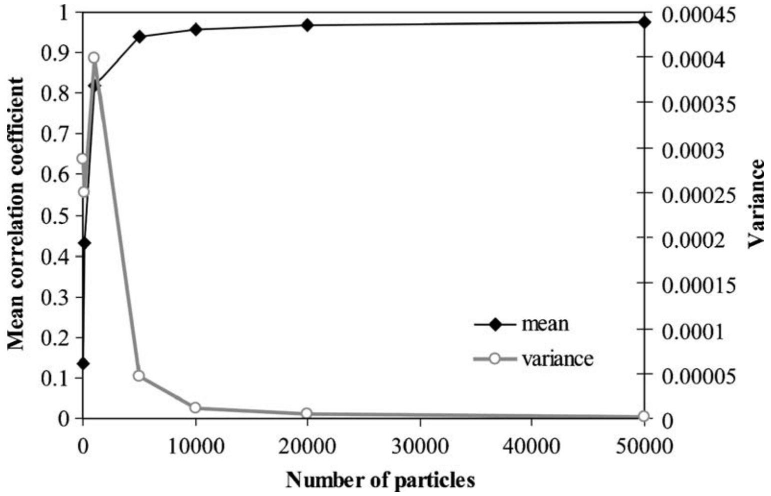

Fig. 4. Dye-release experiments. Mean and variance of model output versus number of particles released. Each mean and variance value was calculated with the Pearson correlation coefficients of particle concentrations versus tracer concentrations at day 352 for 5 simulations of the dye release model. The 5 simulations were conducted with identical models except that different seed values were used to initialize the random number generator.

Particle motion in the *z*-direction was parameterized with a random displacement model implemented with the water column profile interpolation scheme and a 1-s time step. One of 3 levels of smoothing was applied (no smoothing, 4-point moving average, 8-point moving average). It is important to note that shape of the smoothed profile was controlled both by the degree of the moving average and the number of points that were proliferated in the water column profile before smoothing. High numbers of proliferated points (~4 times the number of sigma levels) were used to ensure that smoothed profiles of vertical diffusivity did not deviate substantially from the original profile generated by the hydrodynamic model.

Five simulations were conducted for each gradient value, profile type, and level of smoothing using identical models except that different seed values were used to initialize the random number generator. In each simulation, 4000 randomly distributed particles were released and tracked for 12 h, for a total of 3,960,000 particles in 990 model simulations (2 profile types × 33 gradients × 3 levels of smoothing × 5 seed values).

For the 1D WMC test, the range of particle numbers from profiles of randomly distributed particles was determined (the non-significant range). First, 4000 snapshot distributions of 4000 randomly distributed particles were generated in the 13-m-deep water column. Then, the number of particles was calculated in 28 evenly spaced depth intervals. The highest and lowest value of particle numbers in each depth interval from the 4000 snapshot distributions was used to form the non-significant range. At the end of each 12-h simulation, particle numbers were compared to the non-significant range in each of the 28-m-depth intervals. If particle numbers were within the non-significant range, then particle distributions were not considered different from random distributions and the WMC was satisfied. Otherwise, particle numbers were considered significantly different and indicative of failure of the WMC.

3. Results

3.1. 2D Well Mixed Condition tests

When turbulent particle motion was parameterized with a simple random walk model in the vertical, the particle-tracking model failed the 2D WMC correlation test with a 100% failure rate (Fig. 5). All correlation coefficients were negative and outside the non-significant range and 95% confidence intervals, indicating that high concentrations of particles occurred in areas of low vertical diffusivity as seen in Fig. 2d. According to Wilson and Flesch (1993), if a particle trajectory model fails the WMC, it must do so on the first time increment. In the first 40 s of particle motion, the random walk model failed the 2D WMC test (Table 1).

In contrast, the random displacement model did not fail the 2D WMC test after the first 40 s (Table 1). In fact, 100% of the correlation coefficients remained within the non-significant range and 89% of the correlation coefficients remained within the 95% confidence intervals during the first 7 h of model simulations (Fig. 5b,c). After 7 h, differences in advection

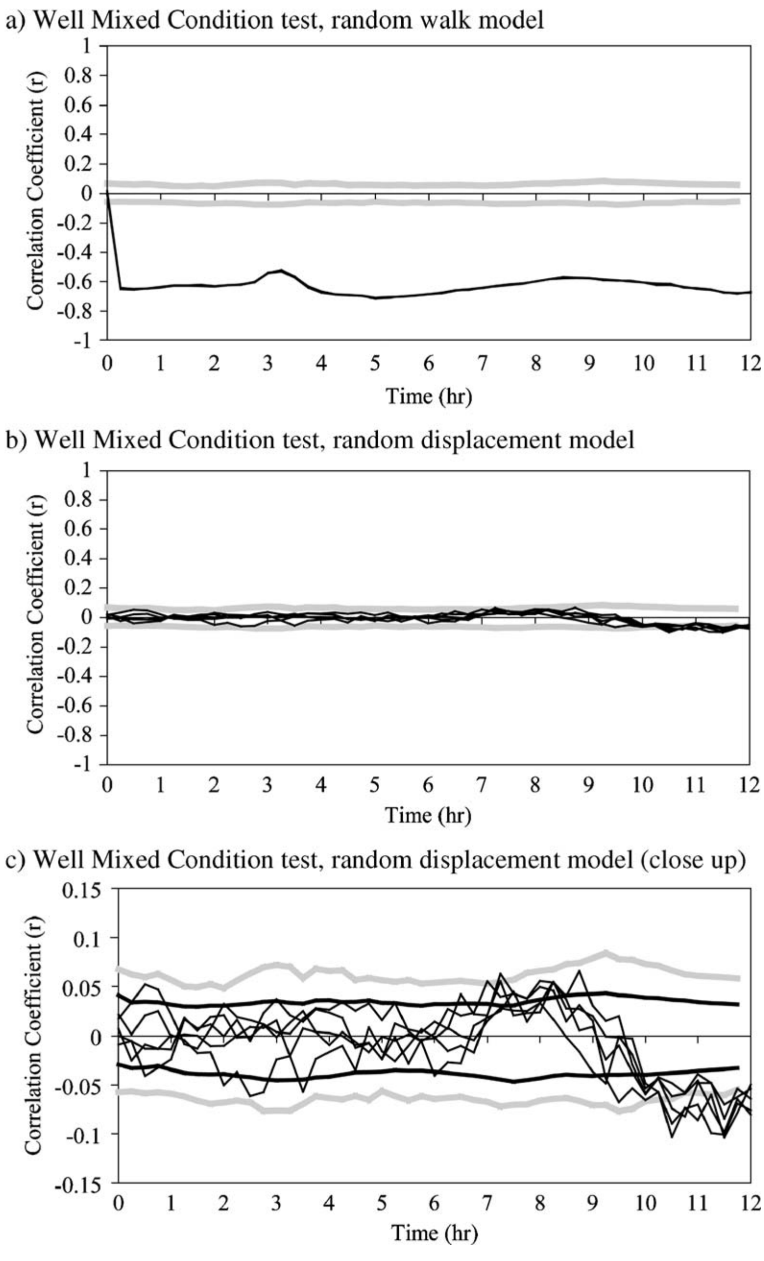

Fig. 5. 2D Well Mixed Condition test. Correlation coefficients of neutrally buoyant particle concentrations versus vertical diffusivity over time for particle-tracking models with different sub-grid scale turbulence models; those with (a) a random walk model and those with (b) a random displacement model. Panel (c) contains the same data as panel (b) but the range of the vertical axis is reduced. Thin black lines are results of models with different initial conditions. Thick black lines in panel (c) represent 95% confidence intervals. Correlation coefficients that do not remain within the non-significant range (thick gray lines) violate the Well Mixed Condition, a necessary condition for simulating unbiased turbulent diffusion in Lagrangian particle-tracking models.

between the upper and lower water column (due to estuarine gravitational circulation), and between the river and seaward boundaries (due to longitudinal changes in tidal current speeds) created differences in particle concentrations near the horizontal boundaries of the particle-tracking model. These gaps and accumulations confounded the WMC tests and resulted in multiple failures toward the end of the 12-h time series. It is apparent that the 95% confidence intervals provide a more stringent test of the WMC than the non-significant range (Fig. 5c). But, it is clear that models that result in massive failures of the WMC do so when

Table 1
2D Well Mixed Condition test results and non-significant range after one hydrodynamic model time step (40 s)

Initial conditions	Correlation coefficients (r)	
	RDM	RWM
A	0.008	−0.228
B	−0.001	−0.233
C	−0.006	−0.251
D	−0.006	−0.235
E	0.021	−0.213
Non-significant range	Upper	Lower
	0.063	−0.057

Correlation coefficients (r) of particle concentrations vs. vertical diffusivities were calculated for particle-tracking models with a random displacement model (RDM) and with a random walk model (RWM) used to simulate turbulent particle motion. Random displacement model and random walk model simulations were repeated 5 times with different initial conditions (lettered A to E). The Well Mixed Condition was demonstrated for the random displacement model because the correlation coefficients were within the non-significant range.

using either the 95% confidence intervals or the non-significant range as criteria.

3.2. Dye-release experiments

In the dye-release experiments, Eulerian tracer and Lagrangian particles were released at the same location up-estuary of the salt front (Fig. 6a) and tracked over time. Contour plots of results from scenarios with (1) neutrally buoyant tracer/particles without a wind event (Fig. 6), and with (2) sinking tracer/particles and a wind event (Fig. 7) are presented herein. In the scenario with neutrally buoyant tracer/particles without a wind event, the neutrally buoyant tracer had diffused both horizontally and vertically, and peak concentrations had advected down-estuary over the salt front, after 4 days (Fig. 6b). Comparison with Lagrangian particle distributions indicated that the particle-tracking model with a random displacement model (Fig. 6c) simulated tracer dispersal more accurately than the particle-tracking model with a random walk model (Fig 6d). The random displacement model simulated the vertical movement and resulting horizontal distribution of particles. In contrast, the random walk model caused particles to rapidly accumulate in areas of low diffusivity (especially near surface), which resulted in transport of particles down-estuary more rapidly than the tracer.

Simulations with sinking particles and tracers confirmed that the random displacement model resulted in more realistic dispersal of particles than the random walk model. Plots of model output after 4 days and a 21-h wind event showed that the tracer peaked in concentration within the tip of the salt front and, to a lesser extent, in the pycnocline (Fig. 7b). The random walk model caused sinking particles to artificially aggregate in areas of low diffusivity near bottom and, most noticeably, in the pycnocline (Fig. 7d). In contrast, the random displacement model resulted in good agreement between particle distributions (Fig. 7c) and tracer concentrations (Fig. 7b).

For all dye-release experiments (neutrally buoyant and sinking tracers/particles, wind and no wind events), correlation coefficients between particle and tracer concentrations indicated close agreement between tracer and particle dispersal over time when the random displacement model was implemented in the particle-tracking model (Fig. 8). One hour after particle and tracer release, correlation coefficients dropped to ~0.8 because the tracer initially spread faster than the particles. But within 6 h, it was clear that correlations between particles and tracer from the random displacement model were high (between 0.84 and 0.99), and were substantially greater than those from the random walk model (between 0.07 and 0.58). In both models, enhanced turbulence during the down-estuary wind event reduced the correlation between tracer and particle concentrations, apparently because the particles were dispersed horizontally slightly faster than the tracer.

3.3. 1D smoothing experiments

Failure of the 1D WMC test was evident in models with gradients in vertical diffusivity that equaled or exceeded $6.9995\times10^{-3}\,m^2\,s^{-1}$ per m (hereafter referred to as $7.0\times10^{-3}\,m^2\,s^{-1}$ per m). For example, Fig. 9 depicts results from 1D WMC test from models with maximum vertical diffusivity of $0.02\,m^2\,s^{-1}$ in the bottom layer. Three failures of the WMC were located in the low diffusivity region just above the sharp gradient in vertical diffusivity and occurred in the model without smoothing in the water column profile interpolation scheme. No failures occurred in the models with smoothing.

Results of all model scenarios combined indicated that smoothing reduced failure of the WMC. Fig. 10 contains plots of the number of failures of 1D WMC tests versus the absolute value of the gradient in vertical diffusivity ($|K'_v|$) in all 1D water column models. The number of failures of the WMC decreased with increasing level of smoothing. When $|K'_v|$ was less than $7.0\times10^{-3}\,m\,s^{-1}$ per m, smoothing of the vertical diffusivity profile was not necessary to maintain the WMC. When $|K'_v|$ was greater than $7.0\times10^{-3}\,m^2\,s^{-1}$ per

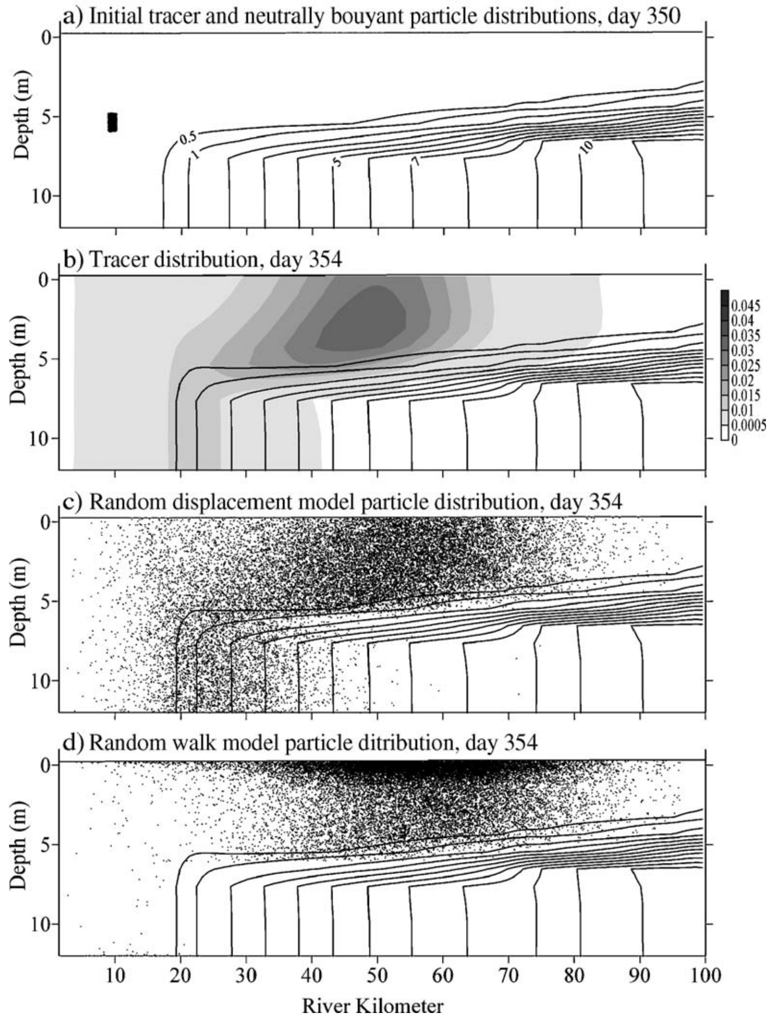

Fig. 6. Dye release studies with neutrally buoyant tracer and particles: (a) initial release location of particles and tracer, (b) tracer distribution after 4 days, (c) particle distribution after 4 days with a random displacement model, and (d) particle distribution after 4 days with a random walk model.

m and less than 1.79995×10^{-2} m s^{-1} per m, then a 4-point moving average was sufficient for the WMC. An 8-point moving average was required to prevent failure of the WMC when $|K_v'|$ was between 1.79995×10^{-2} m s^{-1} and 3.39995×10^{-2} m s^{-1} per m (hereafter referred to as 3.4×10^{-2} m^2 s^{-1} per m). Above 3.4×10^{-2} m^2 s^{-1} per m, failure of the WMC occurred in all models, but was minimized in models with an 8-point moving average.

4. Discussion

Our implementation of a random displacement model within a Lagrangian particle-tracking model successfully simulated turbulent particle motion in a frontal region with sharp gradients in vertical diffusivity. Results clearly supported the findings of Visser (1997) and Brickman and Smith (2002): the random displacement model was much preferred to a random walk model when simulating sub-grid scale turbulence in stratified conditions (compare Fig. 2c with Fig. 2d).

The 'water column profile' interpolation scheme reduced numerical artifacts and allowed attainment of the WMC. Brickman and Smith (2002) suggested that the WMC would not be attainable in ocean circulation models because the low-resolution, discrete output of hydrodynamic models would introduce discontinuities that would prevent demonstration of the WMC (Brickman and Smith, 2002). Our 'water column profile' interpolation scheme offers a way out of this dilemma. It replaced the discrete output with a continuous profile that preserved the shape of the

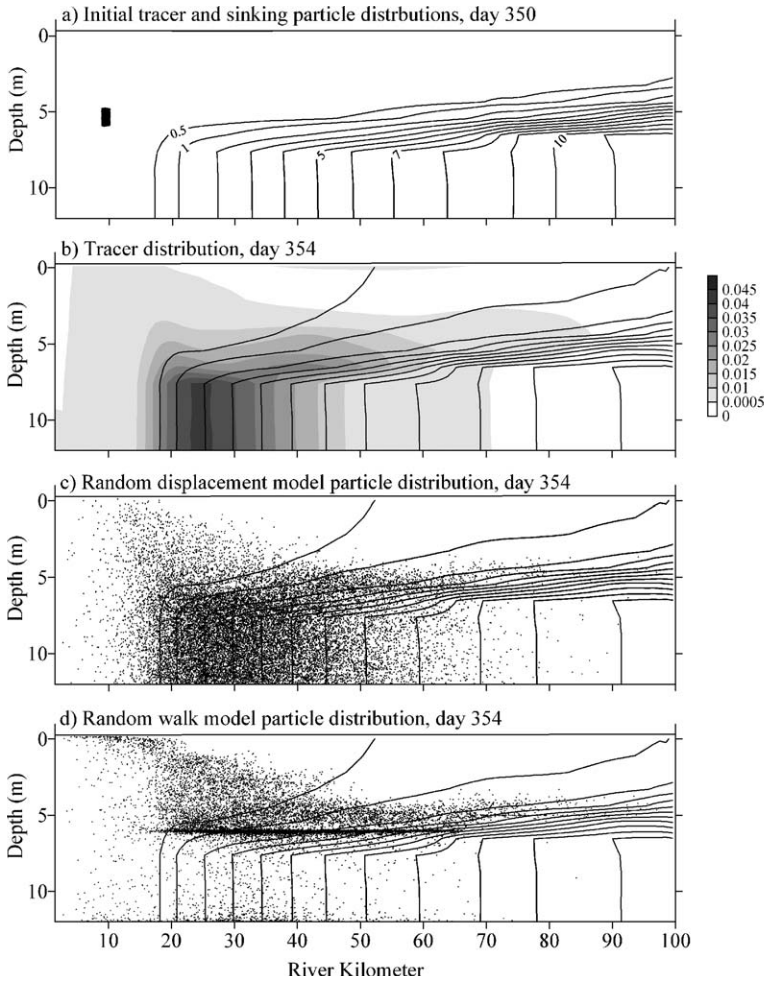

Fig. 7. Dye release studies with sinking tracer and particles, and a 21-h wind event: (a) initial release location of particles and tracer, (b) tracer distribution after 4 days, (c) particle distribution after 4 days with a random displacement model, and (d) particle distribution after 4 days with a random walk model. Sinking particles and tracer were assigned a constant settling velocity of $0.03\,\mathrm{mm\,s^{-1}}$.

data without adding inflection points. It is important to note that constructing a continuous profile of vertical diffusivity was fundamental, but not the only required step, for demonstrating the WMC in the baroclinic salt wedge model. It also was necessary to smooth the vertical diffusivity profile with a moving average. Otherwise, the sharp gradients in vertical diffusivity (e.g., Fig. 3c) caused particles to aggregate at the location where abrupt changes occurred, even when a continuous function was fit to the data.

Although our results are certainly model-dependent, the 1D smoothing experiments suggest that smoothing of the vertical diffusivity profile is necessary in random displacement models implemented in hydrodynamic models with gradients in vertical diffusivity that exceed $7.0\times10^{-3}\,\mathrm{m^2\,s^{-1}}$ per m. Below this value, smoothing may not be required. Field observations in San Francisco Bay estuary indicate that vertical gradients in eddy diffusivity on the order of $1.0\times10^{-2}\,\mathrm{m^2\,s^{-1}}$ per m were present (Stacey et al., 1999). This value is above $7.0\times10^{-3}\,\mathrm{m\,s^{-1}}$ per m and below the value which 8-point linear interpolation fails to maintain the WMC ($3.4\times10^{-2}\,\mathrm{m\,s^{-1}}$ per m). Maximum gradients in vertical diffusivity in the baroclinic salt wedge model ($0.09\,\mathrm{m^2\,s^{-1}}$ per m) were substantially higher than $3.4\times10^{-2}\,\mathrm{m\,s^{-1}}$ per m, but occurred transiently and in isolated portions of the model in steady state conditions. These high values were likely a function of strong density stratification coupled with lack of wind mixing during the 350-day model spin-up. It is likely that the salt wedge model passed the 2D WMC correlation tests even though the 1D WMC tests indicated failure because (1) the high diffusivity values were transient and that the (2) particle motion due to advection and

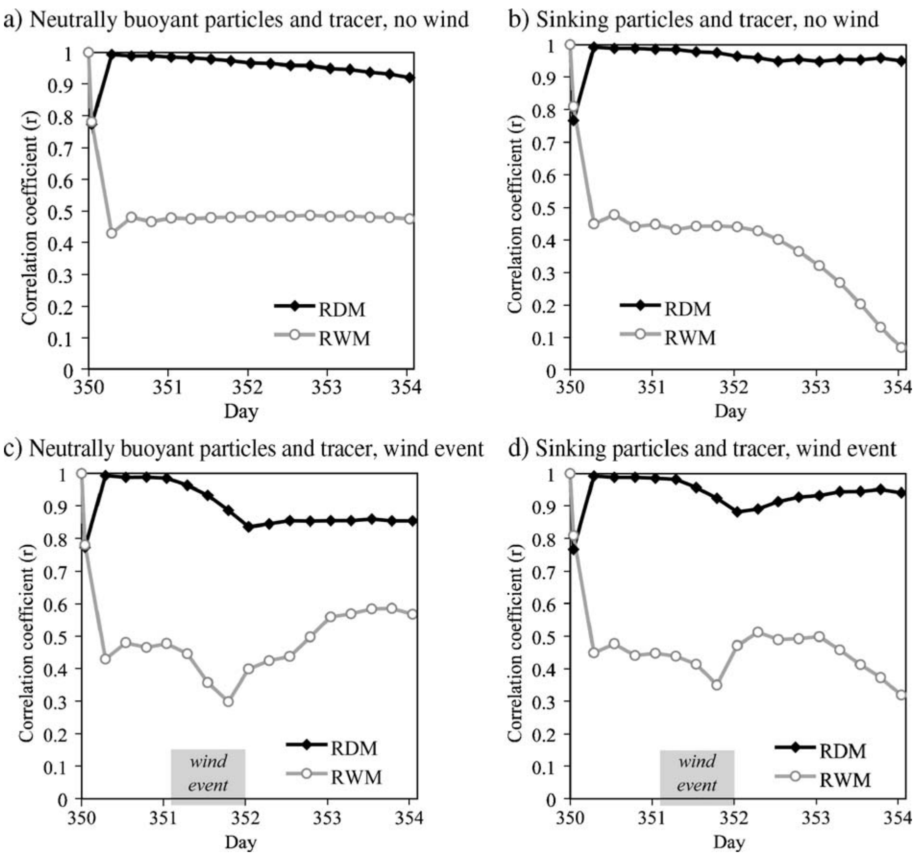

Fig. 8. Dye release studies. Correlation coefficient of particle concentrations vs. Eulerian tracer concentrations over time from models that implement a random displacement model (RDM) or a random walk model (RWM) to simulate turbulent motion of particles. Results are from scenarios with (a, b) tides and river inflow, and (c, d) tides, river inflow and wind, as well as with (a, c) neutrally buoyant particles and (b, d) sinking particles. In scenarios with a wind event, wind stress of 1.66 dyn cm^{-2} was imposed from day 351.125 to 352 (21 h). A shaded box indicates timing of the wind event. Sinking particles and tracer were assigned a constant settling velocity of 0.03 mm s^{-1}.

horizontal mixing was included in the salt wedge model and may have rapidly dispersed particle accumulations if they occurred.

The random displacement model presented here passed the both the 1D and 2D WMC tests despite the fact that simple surface and bottom boundary conditions were implemented. According to Wilson and Flesch (1993), reflective boundary conditions should result in the violation of the WMC in models with inhomogeneous turbulence. In addition, Brickman and Smith (2002) reported that theoretical work indicated that the gradient in vertical diffusivity should be zero at model boundaries in order to demonstrate the WMC. Yet, when we conducted 2D model scenarios with the gradient in K_v forced to zero at the boundaries, this parameterization did not improve particle-tracking model performance (not shown). Instead, we found that demonstration of the WMC was influenced by (1) the interpolation scheme used to estimate K_v', and (2) the time step of the particle-tracking model. When the time step of the particle-tracking model was equal to that of the hydrodynamic model (40 s), failure of the 2D WMC increased. This was likely due to transient accumulations of particles near the surface and bottom boundaries within the region of the frontal convergence zone, or potentially where $|K_v'|$ exceeded 3.4×10^{-2} m s^{-1} per m. As suggested by Proehl and Lynch (2001), increasing the temporal resolution of the particle-tracking model (to 10 s) appeared to alleviate this problem. In addition, it is likely that the short time step of the random displacement model (1 s) allowed attainment of the WMC, despite the use of simple boundary conditions.

Results of the dye-release experiments indicated good agreement between Eulerian and Lagrangian techniques for simulating dispersal when the random displacement model was implemented. The random walk model was clearly inadequate; it resulted in artificial aggregation of particles in regions of low

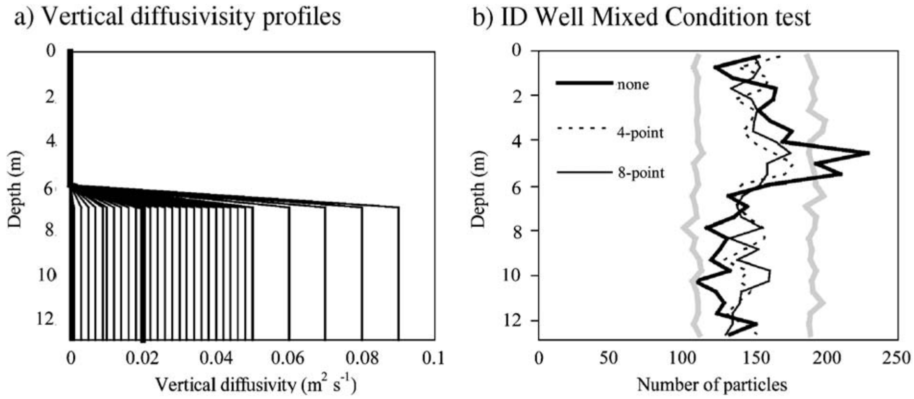

Fig. 9. 1D smoothing experiments. (a) Vertical diffusivity profiles used in models with highest diffusivities in bottom layer. Minimum vertical diffusivity was $5.0\times10^{-7}\,m^2\,s^{-1}$ in all profiles. Darkened line represents the profile used to generate model results presented in panel (b). (b) Results of 1D Well Mixed Condition tests of models with maximum vertical diffusivity of $0.02\,m^2\,s^{-1}$ and random displacement models that had no smoothing (thick black line), smoothing with a 4-point moving average (dashed line), and smoothing with an 8-point moving average (thin black line) in the water column profile interpolation scheme. Particle numbers that are outside the non-significant range (thick gray lines) violate the Well Mixed Condition.

vertical diffusivity near surface and bottom boundaries, and within the pycnocline. Although the random displacement model was able to simulate the motion of both neutrally buoyant and sinking tracers, its performance decreased during the down-estuary wind event (Fig. 8c,d). Note the model formulations for particles and tracers differ substantially in details. A logarithmic bottom boundary layer was explicitly incorporated in the particle component but poorly resolved in the tracer component. Further, the vertical diffusivity was reconstituted in the particle component and therefore deviates somewhat from that in the tracer component. The cumulative effect of these minor differences could contribute to the slight discrepancy.

In general, results of the model performance tests indicated that the coupled hydrographic–Lagrangian model successfully simulated turbulent particle motion and dispersal in a strongly baroclinic frontal region. We suggest that the random displacement model coupled with the 'water column profile' interpolation scheme allows simulation of particle motion in frontal regions that heretofore has been limited by numerical artifacts. In addition, the water column profile scheme is appropriate for models with irregular bathymetry and non-uniform grids because interpolation takes place along sigma-levels and is independent of grid cell shape. As such, the modeling framework presented here has the potential to be a useful tool for investigating the

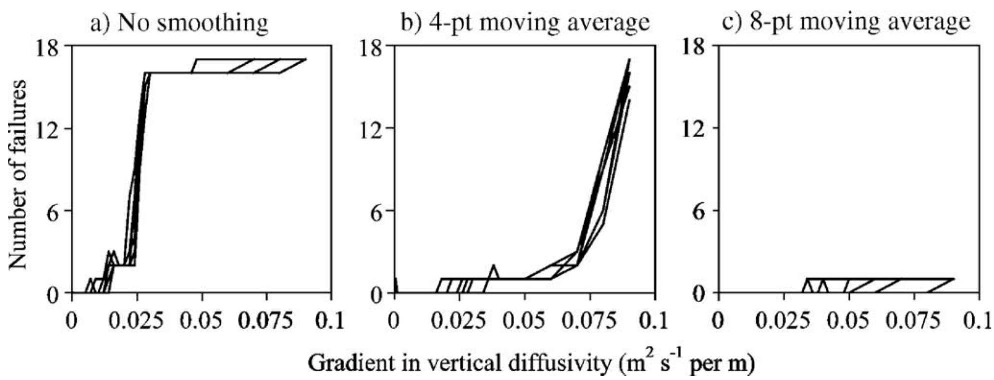

Fig. 10. 1D smoothing experiments. Number of failures of Well Mixed Condition tests versus the absolute value of the gradient in vertical diffusivity ($|K_v'|$, $m^2\,s^{-1}$ per m) in 1D water column models. In these models, the random displacement model was implemented with a water column profile interpolation scheme (a) without smoothing of the vertical diffusivity profile, (b) with smoothing by a 4-point moving average, and (c) with smoothing by an 8-point moving average. Thin black lines are results of models with the same $|K_v'|$ but (1) different seed values used to initialize the random number generator and (2) different locations for maximum diffusivity values (either surface or bottom layers).

influence of hydrographic variability on sediment particles and biological–physical interactions in estuarine and coastal frontal zones.

Acknowledgements

We thank Charles Hannah, Uffe Thygesen, and Tipani Stipa for helpful advice and discussions. EN appreciates the forum provided by the ICES Study Group on Modeling Physical–Biological Interactions, and NSF support, which facilitated these discussions. This research was part of the Bio-Physical Interactions in the Turbidity Maximum (BITMAX) program sponsored by an NSF Biological Oceanography Program award to SYC, RRH, LPS, E. D. Houde, M. R. Roman, and C. T. Friedrichs (Grant No.: OCE-0002543). This is UMCES contribution no. HPL-3875.

References

Allen, G.P., Salomon, J.C., Bassoullet, P., Du Penhoat, Y., De Grandpré, C., 1980. Effects of tides on mixing and suspended sediment in macrotidal estuaries. Sediment Geology 26, 69–80.

Bartsch, J., Coombs, S.H., 2001. An individual-based growth and transport model of the early life-history stages of mackerel (*Scomber scombrus*) in the eastern North Atlantic. Ecological Modeling 138, 127–141.

Bennett, W.A., Kimmerer, W.J., Burau, J.R., 2002. Plasticity in vertical migration by native and exotic estuarine fishes in a dynamic low-salinity zone. Limnology and Oceanography 47 (5), 1496–1507.

Bjorkstedt, E.P., Rosenfeld, L.K., Grantham, B.A., Shkedy, Y., Roughgarden, J., 2002. Distributions of larval rockfishes *Sebastes* spp. across nearshore fronts in a coastal upwelling region. Marine Ecology Progress Series 242, 215–228.

Blumberg, A.F., Mellor, G.L., 1987. A description of a three-dimensional coastal ocean circulation model. In: Heaps, N. (Ed.), Three-Dimensional Coastal Ocean Models. American Geophysical Union, Washington, D.C.

Boynton, W.R., et al., 1997. Interactions Between Physics and Biology in the Estuarine Turbidity Maximum (ETM) of Chesapeake Bay, USA. International Council for the Exploration of the Sea. CM 1997/S:11.

Brickman, D., Smith, P.C., 2002. Lagrangian stochastic modeling in coastal oceanography. Journal of Atmospheric and Ocean Technology 19, 83–99.

Brown, C.A., Holt, S.A., Jackson, G.A., Brooks, D.A., Holt, G.J., 2004. Simulating larval supply to estuarine nursery areas: how important are physical processes to the supply of larvae to the Aransas Pass Inlet? Fisheries Oceanography 13, 181–196.

Burau, J.R., Gartner, J.W., Stacey, M., 1998. Results from the hydrodynamic element of the 1994 entrapment zone study in Suisun Bay. In: Kimmerer, W. (Ed.), Report of the 1994 Entrapment Zone Study. Interagency Ecological Program for the San Francisco Bay/Delta Estuary.

D'Anglejan, B., 1981. On the advection of turbidity in the Saint Lawrence middle estuary. Estuaries 4 (10), 2–15.

Dauvin, J.C., Dodson, J.J., 1990. Relationship between feeding incidence and vertical and longitudinal distribution of rainbow smelt larvae (*Osmerus mordax*) in a turbid well-mixed estuary. Marine Ecology–Progress Series 60 (1–2), 1–12.

Dodson, J.J., Dauvin, J.C., Ingram, R.G., Dangeljan, B., 1989. Abundance of larval rainbow smelt (*Osmerus mordax*) in relation to the maximum turbidity zone and associated macroplanktonic fauna of the Middle St Lawrence Estuary. Estuaries 12 (2), 66–81.

Epifanio, C., 1987. The role of tidal fronts in maintaining patches of *Brachyuran zoeae* in estuarine waters. Journal of Crustacean Biology 7 (3), 513–517.

Epstein, A.W., Beardsley, R.C., 2001. Flow-induced aggregation of plankton at a front: a 2-D Eulerian model study. Deep-Sea Research Part Ii–Topical Studies in Oceanography 48 (1–3), 395–418.

Franks, P.J.S., Walstad, L.J., 1997. Phytoplankton patches at fronts: a model of formation and response to wind events. Journal of Marine Research 55, 1–29.

Geyer, W.R., Woodruff, J.D., Traykovski, P., 2001. Sediment transport and trapping in the Hudson River estuary. Estuaries 24 (5), 670–679.

Govoni, J.J., 1993. Flux of larval fishes across frontal boundaries: examples from the Mississippi River plume front and the western Gulf Stream front in winter. Bulletin of Marine Science 52 (2), 538–566.

Govoni, J.J., Grimes, C.B., 1992. The surface accumulation of larval fishes by hydrodynamic convergence within the Mississippi River plume front. Continental Shelf Research 12 (11), 1265–1276.

Govoni, J.J., Hoss, D.E., Colby, D.R., 1989. The spatial distribution of larval fishes about the Mississippi River plume. Limnology and Oceanography 34 (1), 178–187.

Hannah, C.G., Naimie, C.E., Loder, J.W., Werner, F.E., 1998. Upper-ocean mechanisms from the Gulf of Maine to Georges Bank, with implications for *Calanus* supply. Continental Shelf Research 17 (15), 1887–1911.

Hare, J.A., et al., 1999. Larval transport during winter in the SABRE study area: results of a coupled vertical behavior–three-dimensional circulation model. Fisheries Oceanography 8 (Supplement 2), 57–76.

Heath, M.R., Gallego, A., 1998. Bio-physical modelling of the early life stages of haddock, *Melanogrammus aeglefinus*, in the North Sea. Fisheries Oceanography 7 (2), 110–125.

Hinckley, S., Hermann, A.J., Mier, K.L., Megrey, B.A., 2001. Importance of spawning location and timing to successful transport to nursery areas: a simulation study of Gulf of Alaska walleye pollock. ICES Journal of Marine Science 58, 1042–1052.

Hinrichsen, H.H., Bottcher, U., Koster, F.W., Lehmann, A., St John, M.A., 2003. Modelling the influences of atmospheric forcing conditions on Baltic cod early life stages: distribution and drift. Journal of Sea Research 49, 187–201.

Hood, R.R., Abbott, M.R., Huyer, A., 1991. Phytoplankton and photosynthetic light response in the coastal transition zone off northern California in June 1987. Journal of Geophysical Research Oceans 96 (C8), 14769–14780.

Hood, R.R., Wang, H.V., Purcell, J.E., Houde, E.D., Harding Jr., L.W., 1999. Modeling particles and pelagic organisms in Chesapeake Bay: convergent features control plankton distributions. Journal of Geophysical Research (Oceans) 104 (C1), 1223–1243.

Jassby, A.D., et al., 1995. Isohaline position as a habitat indicator for estuarine populations. Ecological Applications 5 (1), 272–289.

Jay, D.A., Musiak, J.D., 1994. Particle trapping in estuarine tidal flows. Journal of Geophysical Research 99 (C10), 20,445–20,461.

Jillett, J.B., Zeldis, J.R., 1985. Aerial observations of surface patchiness of a planktonic crustacean. Bulletin of Marine Science 37 (2), 609–619.

Kappenberg, J., Grabemann, I., 2001. Variability of the mixing zones and estuarine turbidity maxima in the Elbe and Weser estuaries. Estuaries 24 (5), 699–706.

Kingsford, M.J., Suthers, I.M., 1996. The influence of tidal phase on patterns of ichthyoplankton abundance in the vicinity of an estuarine front, Botany Bay, Australia. Estuarine, Coastal and Shelf Science 43 (1), 33–54.

Kostaschuk, R., 2002. Flow and sediment dynamics in migrating salinity intrusions: Fraser River estuary, Canada. Estuaries 25 (2), 197–203.

Largier, J.L., 1993. Estuarine fronts: how important are they? Estuaries 16 (1), 1–11.

Lin, J., Kuo, A.Y., 2001. Secondary turbidity maximum in a partially mixed microtidal estuary. Estuaries 24 (5), 707–720.

Lough, R.G., Manning, J.P., 2001. Tidal-front entrainment and retention of fish larvae on the southern flank of Georges Bank. Deep Sea Research II 48, 631–644.

Mackas, D.L., Louttit, G.C., 1988. Aggregation of the copepod *Neocalanus plumchrus* at the margin of the Fraser River plume in the Strait of Georgia. Bulletin of Marine Science 43 (3), 810–824.

Mellor, G.L., 1998. User's Guide for a Three-Dimensional, Primitive Equation, Numerical Ocean Model. . Program in Atmospheric and Ocean Sciences. Princeton University, Princeton, New Jersey.

Mellor, G.L., Yamada, T., 1974. A hierarchy of turbulence closure models for planetary boundary layers. Journal of Atmospheric Science 31, 1791–1806.

Munk, P., Larsson, P.O., Danielssen, D.S., Moksness, E., 1999. Variability in frontal zone formation and distribution of gadoid fish larvae at the shelf break in the northeastern North Sea. Marine Ecology Progress Series 177, 221–233.

Munk, P., Wright, P.J., Pihl, N.J., 2002. Distribution of the early larval stages of cod, plaice and lesser sandeel across haline fronts in the North Sea. Estuarine, Coastal and Shelf Science 55 (1), 139–149.

Nakata, H., Kimura, S., Okazaki, Y., Kasai, A., 2000. Implications of mesoscale eddies caused by frontal disturbances of the Kuroshio Current for anchovy recruitment. ICES Journal of Marine Science 57 (1), 143–152.

North, E.W., Houde, E.D., 2001. Retention of white perch and striped bass larvae: biological–physical interactions in Chesapeake Bay estuarine turbidity maximum. Estuaries 24 (5), 756–769.

North, E.W., Houde, E.D., 2003. Linking ETM physics, zooplankton prey, and fish early-life histories to white perch (*Morone americana*) and striped bass (*M. saxatilis*) recruitment success. Marine Ecology Progress Series 260, 219–236.

North, E.W., Houde, E.D., 2004. Transport and dispersal of bay anchovy (*Anchoa mitchilli*) eggs and larvae in Chesapeake Bay. Estuarine. Coastal and Shelf Science 60, 409–429.

North, E.W., Chao, S.Y., Sanford, L.P., Hood, R.R., 2004. The influence of wind and river pulses on an estuarine turbidity maximum: numerical studies and field observations. Estuaries 27 (1), 132–146.

Okazaki, Y., Nakata, H., Iwatsuki, Y., 1998. Distribution and food availability of fish larvae in the vicinity of a thermohaline front at the entrance of Ise Bay. Fisheries Science 64 (2), 228–234.

Proehl, J.A., Lynch, D.R., 2001. Experiments in Lagrangian diffusion. Report #NML-01-5, Numerical Methods Laboratory. Dartmouth College, Dartmouth. 16 pp.

Roman, M., Zhang, X., McGilliard, C., Boicourt, W., 2005. Seasonal and annual variability in the spatial patterns of plankton biomass in Chesapeake Bay. Limnology and Oceanography 50 (2), 480–492.

Sanford, L.P., Suttles, S.E., Halka, J.P., 2001. Reconsidering the physics of the Chesapeake Bay estuarine turbidity maximum. Estuaries 24 (5), 655–669.

Schubel, J.R., 1968. Turbidity maximum of northern Chesapeake Bay. Science 161 (3845), 1013–1015.

Shanks, A.L., Largier, J., Brink, L., Brubaker, J., Hooff, R., 2000. Demonstration of the onshore transport of larval invertebrates by the shoreward movement of an upwelling front. Limnology and Oceanography 45 (1), 230–236.

Sirois, P., Dodson, J.J., 2000. Influence of turbidity, food density and parasites on the ingestion and growth of larval rainbow smelt *Osmerus mordax* in an estuarine turbidity maximum. Marine Ecology–Progress Series 193, 167–179.

Stacey, M.T., Monismith, S.G., Burau, J.R., 1999. Observations of turbulence in a partially stratified estuary. Journal of Physical Oceanography 29 (8), 1950–1970.

Uncles, R.J., Stephens, J.A., 1993. The freshwater–saltwater interface and its relationship to the turbidity maximum in the Tamar estuary, United Kingdom. Estuaries 16 (1), 126–141.

Uye, S.-I., Yamaoka, T., Fujisawa, T., 1992. Are tidal fronts good recruitment areas for herbivorous copepods? Fisheries Oceanography 1 (3), 216–226.

Visser, A.W., 1997. Using random walk models to simulate the vertical distribution of particles in a turbulent water column. Marine Ecology Progress Series 158, 275–281.

Werner, F.E., et al., 2001. Larval trophodynamics, turbulence, and drift on Georges Bank: a sensitivity analysis of cod and haddock. Scientia Marina 65, 99–115.

Werner, F.E., Perry, R.I., Lough, R.G., Naimie, C.E., 1996. Trophodynamic and advective influences on Georges Bank larval cod and haddock. Deep-Sea Research 43 (7–8), 1793–1822.

Wilson, J.D., Flesch, T.K., 1993. Flow boundaries in random-flight dispersion models: enforcing the Well-Mixed Condition. Journal of Applied Meteorology 32, 1695–1707.

Winkler, G., Dodson, J.J., Bertrand, N., Thivierge, D., Vincent, W.F., 2003. Trophic coupling across the St. Lawrence River estuarine transition zone. Marine Ecology–Progress Series 251, 59–73.

Wolanski, E., Hamner, W.M., 1988. Topographically controlled fronts in the ocean and their biological influence. Science 241, 177–181.